Opto-Electronic Advances

Review

2018, Vol. 1, No. 2

DOI: 10.29026/oea.2018.170002

Diffractive photonic applications mediated by laser reduced graphene oxides

Sicong Wang[1], Xueying Ouyang[1], Ziwei Feng[1], Yaoyu Cao[1], Min Gu[2]* and Xiangping Li[1]*

Modification of reduced graphene oxide in a controllable manner provides a promising material platform for producing graphene based devices. Its fusion with direct laser writing methods has enabled cost-effective and scalable production for advanced applications based on tailored optical and electronic properties in the conductivity, the fluorescence and the refractive index during the reduction process. This mini-review summarizes the state-of-the-art status of the mechanisms of reduction of graphene oxides by direct laser writing techniques as well as appealing optical diffractive applications including planar lenses, information storage and holographic displays. Owing to its versatility and up-scalability, the laser reduction method holds enormous potentials for graphene based diffractive photonic devices with diverse functionalities.

Keywords: graphene oxides; nanophotonics; direct laser writing

Wang S C, Ouyang X Y, Feng Z W, Cao Y Y, Gu M *et al*. Diffractive photonic applications mediated by laser reduced graphene oxides. *Opto-Electronic Advances* **1**, 170002 (2018).

Introduction

Graphene[1, 2], an allotrope of hexagonal lattice carbon materials with peculiar electronic and optical properties, emerges as an entirely new material platform for rapid developments of advanced optoelectronic devices. Graphene oxide (GO) known as a disordered analogue of graphene, is attracting intense research efforts owing to its appealing characteristics and the capability of conversion back to graphene[3, 4]. The atomic structure of reduced graphene oxide (rGO) is similar to that of graphene except decorated with structural defects and residual oxygen-containing groups. Therefore, rGO emerges as a straightforward approach for scalable and facile production of graphene-based materials even though it exhibits slightly different electronic and optical properties. In this regard, it has compelled onrushing developments of reduced-graphene-oxide-based devices including flexible circuits[5-7], super-capacitors[8-10], sensors[11,12], planar lenses[13], information storage and displays[14,15].

The atomic structure of GO is different from graphene. Even though with disorder and presence of defects due to oxygen-containing species at the edges or at the basal plane, the hexagonal lattice of crystalline graphene is preserved in GO[16-18], as illustrated in Fig. 1. As a consequence, a unique set of physical characteristics stems

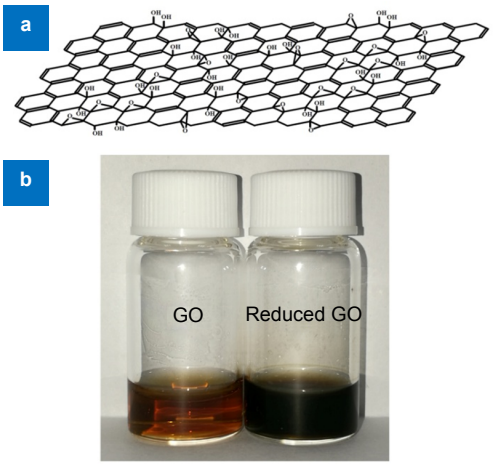

Fig. 1 | (**a**) The chemical structure of a monolayer graphene oxide adapted from the Lerf-Klinowski model. (**b**) GO flakes prepared in water solution exhibit brown color before photoreduction and transform into dark color after photoreduction. Figure reproduced from (**a**) ref. [18], Elsevier Science B.V.

[1]Guangdong Provincial Key Laboratory of Optical Fiber Sensing and Communications, Institute of Photonics Technology, Jinan University, Guangzhou 510632, China; [2]Laboratory of Artificial-Intelligence Nanophotonics and CUDOS (Centre for Ultrahigh bandwidth Devices for Optical Systems), School of Science, RMIT University, Melbourne, Victoria 3001, Australia

* Correspondence: X P Li, E-mail: xiangpingli@jnu.edu.cn; M Gu, E-mail: min.gu@rmit.edu.au

Received 21 December 2017; accepted 23 January 2018; accepted article preview online 12 February 2018

from the mixture of sp2 and sp3 hybridization. During the reduction process of GO, the absence of oxygen groups leads to the creation of new sp2 clusters and partly recovers optoelectronic properties of graphene. In particular, tailoring the electronic and optical properties of rGO through a variety of reduction methods has aroused a research upsurge by precisely manipulating reduction extents of GO[19-21]. In stark contrast to existing reduction methods by reactive chemicals and heat, direct laser reduction is particularly intriguing as it allows in-situ and one-step fabrications of rGO-based devices by removing the necessity of additional transfer of rGO films to the substrate. Most importantly, it enables tunable optoelectronic properties of rGO with a high spatial resolution by precisely controlling the extent of reduction, thus making it a flexible approach for various optical applications with diverse functionalities.

Even though tremendous progresses have been made in producing laser-reduced GO as well as its applications to various optoelectronic devices[5-10], the understanding of the interactions between laser beams and GO is still in its infancy. In addition, the chemistry and atomic structure of GO are much more complex than the monolayer graphene, with a wide variability of species and distribution of the defects. More optoelectronic devices or applications with advanced functionalities based on rGO are yet to be demonstrated. Nevertheless, great endeavors have been devoted to novel applications of laser-reduced GO. In this article, the recent progress specific to laser-reduced GO is reviewed. Firstly, optical properties of GO and rGO are discussed in addition to their characterization methods. Secondly, fundamentals and mechanisms of laser reduction of GO are discussed in details. Finally, we survey the recent work of photonic applications based on laser-reduced GO.

Optical properties and characterization of rGO

Fundamentally different from graphene, the oxygen-containing-group-induced heterogeneous atomic and electronic structures in GO and rGO lead to inconceivable optical properties, denoting a broad fluorescent emission band in the visible range[22-24]. It is generally believed that the fluorescence emission in GO and rGO is mainly ascribed to the recombination of electron-hole pairs in localized states due to the presence of oxygen-based defects, rather than from band-edge transitions in typical semiconductors[19,24]. The fluorescence in GO can be tunable from ultraviolet to near infrared depending on the size of sp2 clusters[19,24], and the quantum efficiency can be as high as 6.9%[25]. The reduction of GO is able to partly recover the structure of graphene by removing oxygen-containing functional groups, which gives rise to a reduced fluorescence intensity, as shown in Fig. 2a. Even though the insights into the mechanisms of fluorescence in GO remain unclear, the tunable fluorescence from GO opens up a number of exciting optical applications for graphene-based materials[22].

The investigation into the linear dispersion of monolayer GO and rGO remains sparse. In addition to the complexity of their atomic structures, the interlayer interactions between covalently bonded oxygen-containing groups restrain the insights into the linear dispersion of monolayers. Nevertheless, the linear dispersion relations have been experimentally studied in GO and rGO thin films composed of multilayers of nano-flakes[26]. GO film shows an almost dispersionless feature with a refractive index around 2.0 and a constant extinction coefficient above 400 nm. The strong interband absorption in the UV range leads to a drastic decrease in refractive index and a notable rise in the extinction coefficient. During the reduction process, increased relative fractions of sp2 clusters, changes of the electronic structure, and hence the modulations of optical properties are direct consequence of the removal of oxygen-containing groups. As shown in Fig. 2b, the conversion from GO to rGO results in a remarkable increase in the refractive index and the extinction coefficient which generally resembles graphene.

Raman spectroscopy is an indispensable and noninvasive method to study the atomic structure, chemical bonds and disorder of rGO[27]. Generally, three distinctive peaks around to D (1333 cm^{-1}), G (1578 cm^{-1}) and 2D (2682 cm^{-1}) modes, respectively, are the prominent features in the Raman spectrum of graphene and its derivatives. The D band is sensitive to the structural disorder in sp2 hybridized carbon systems, which is widely utilized to characterize the level of disorder in graphene, while the G band denotes Raman signature of the vibration of sp2 bonded carbon atoms. The 2D mode is the most salient signature in single-layer graphene, which is not a common characteristic in rGO. Hereby, the relative ratio between the D and G modes (I_D/I_G) is widely utilized as a reliable recognition of reduction of GO, as shown in Fig. 2c. Since the electrical and optical properties of GO and rGO are largely determined by the sp2 π-electron scarbon networks[28], additional recognition of the fraction of sp2 bonding can be provided by X-ray photoelectron spectrometry (XPS) for insights into structure-property relationships during the reduction process[29]. Figure 2d depicts a typical example of XPS results for GO before and after reduction. The deoxygenation by the reduction process can be evidently observed through a remarkable suppression of the C–O–C (286 eV), C=O (287 eV) and OH–C=O (288.5 eV) bonds, which implies a partial restoration of the pure C–C/C=C bond towards graphene.

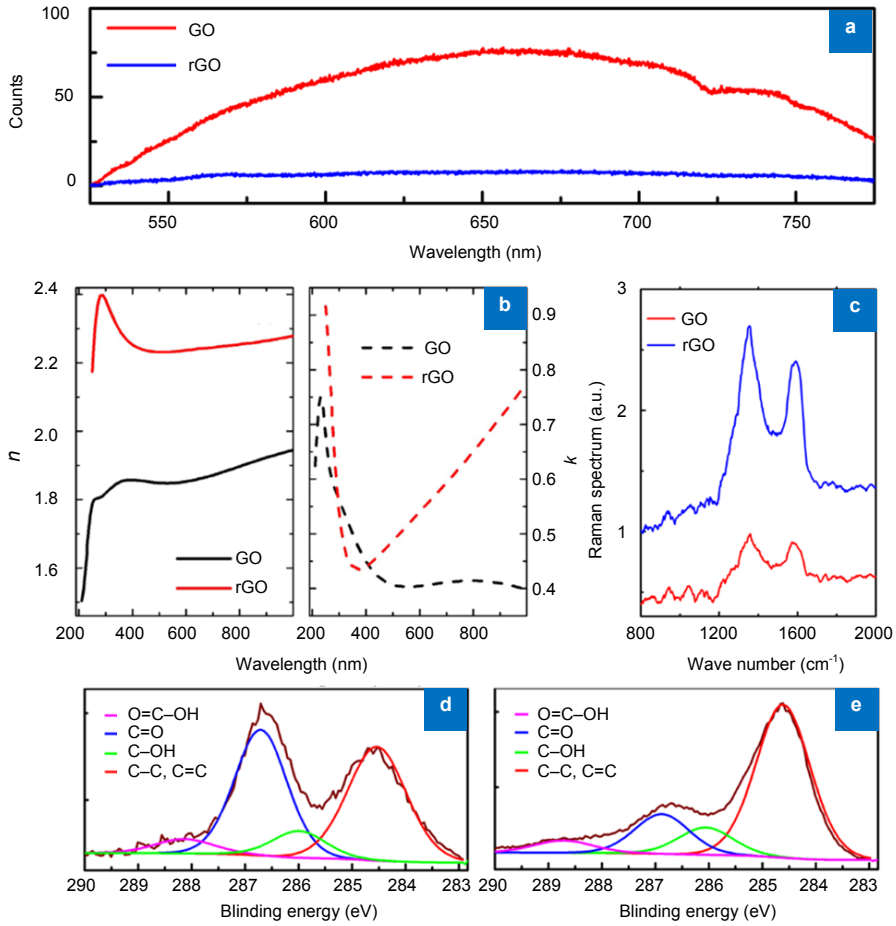

Fig. 2 | (**a**) GO exhibits a broadband fluorescence emission ranging from 550 nm to 750 nm. rGO displays similar fluorescence emission but with a reduced intensity. (**b**) Dispersion relations of refractive indices and extinction coefficients of GO and rGO films. (**c**) Raman spectra of GO before and after reduction exhibit prominent peaks at D (1354 cm^{-1}) and G (1599 cm^{-1}) bands. XPS spectra of GO before (**d**) and after reduction (**e**). Figure reproduced from: (**a**, **c**) ref. [14], Nature Publishing Group; (**b**) ref. [26], IOP Publishing; (**d**, **e**) ref. [15], Springer Nature.

Direct laser reduction

The reduction of GO by chemical reagents such as hydrazine was reported even before the discovery of graphene[30]. Reduction by strong reductants of different species provides a cost-effective and facile method for the scalable production of rGO. Alternative approach to eliminate the oxygen-containing groups in GO and massively produce rGO is heat treatment. Researches show that the reduction of GO can be achieved once the temperature exceeds 200 ℃[31,32], and moreover, the reduction extent can be enlarged by elevating the reaction temperature. However, these methods generally involve multiple steps in the fabrication of rGO-based devices as additional transfer from the rGO film to the substrate is imperative, which trammels their device applications.

A high-temperature deoxygenation process can also be achieved by direct laser reduction including continuous wave (CW) or pulsed laser illuminations at high repetition rates, which enables to produce rGO and simultaneously pattern rGO-based devices (Fig. 3). Irradiated by a CW laser beam at the wavelength of 633 nm multi-layer rGO under nitrogen protection has been obtained with the DLW technique[33]. The absorbed photon can be efficiently converted into heat for a focal temperature rise exceeding a few hundred degrees, which leads to the decomposition of oxygen-containing groups. Patterning GO while simultaneous photothermal reduction can also be realized at the focus of helium ion beams at ambient environment with the maskless laser lithography technique[34]. Later, a facile LightScribe method by a DVD optical drive operating at the near infrared wavelength of 788 nm was successfully employed to reduce GO and even make greyscale patterns[8,35]. However, strong photothermal effect induced by the tightly focused CW beams often diffuses out of the focal region, which leads to the characteristic reduction size on the order of tens of microns significantly larger than the diffraction-limited region.

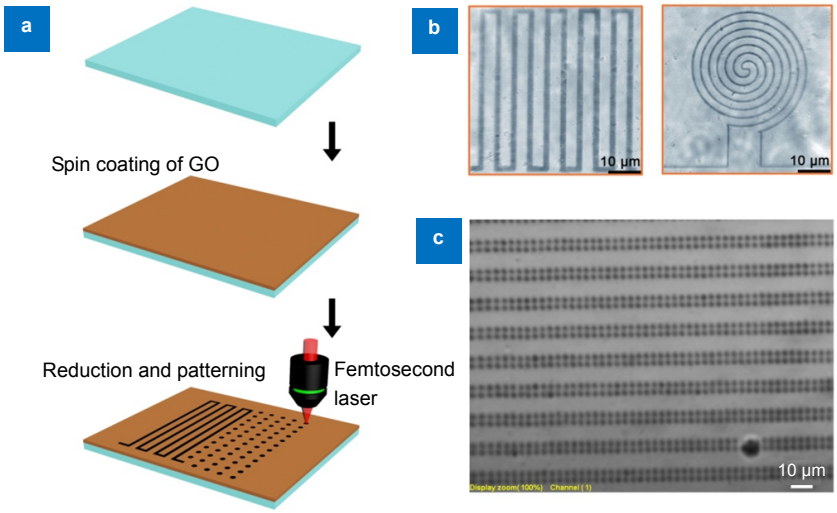

Fig. 3 | (**a**) Schematic illustration of photoreduction and patterning of GO through direct laser writing techniques. Optical microscopic images of patterned rGO samples by femtosecond-pulsed laser beams with a high repetition rate of 80 MHz (**b**) and highly spatially confined reduction by single femtosecond pulses (**c**). Figure reproduced from: (**b**) ref. [6], Elsevier.

Microscale or nanoscale rGO-based devices with advanced functionalities generally require complex patterns demanding fabrication with high spatial resolution and fine feature sizes. In this regard, a high-repetition-rate pulsed laser beam can produce cumulative heating effects only within the confined focal region and hence make pattering rGO with an improved spatial resolution, which emerges as an expanding research topic. Based on a numerical modeling of accumulative temperature effects, the focal temperature of GO can be raised up by 500 ℃ by successive laser pulses at a fluence of ~2 nJ/cm^2 within a few milliseconds, which suffices to initiate the reduction of GO[15]. The reduction of GO under nitrogen protection irradiated by intense picosecond pulsed beams has been investigated at the wavelength of 1064 nm[36]. In particular, a remarkably improved feature size of 500 nm of the patterned rGO circuits could be achieved by using quasi- continuous (repetition rate = 80 MHz) focused femtosecond pulses at the wavelength of 790 nm[6].

In general, electronic excitation effect by absorbing the ultrashort femtosecond pulse is prompt and dominant in the first several picoseconds, which weakens the C–O bonds close to the top of the valence band and triggers the subsequent deoxygenation process. The non-radiative relaxation of carriers introducing thermal effects takes place after 100 picoseconds approximately. Thus, in principle, athermal photoreduction of GO by a single ultrashort pulse is possible as long as the photon is energetic enough beyond the reduction threshold around 3.2 eV[37] and hence cumulative thermal effects can be temporally eliminated. Based on this expectation, single femtosecond pulse induced athermal photoreduction of GO at subwavelength scale through a nonlinear-absorption process has been successfully demonstrated[15]. In order to verify the athermal nature of the observed photoreduction, spherical fluorescent CdSe nanoparticles were employed as nanothermometers to monitor the temperature increase within the focal region. The electronic excitation nature by ultra-short single pulses cannot only restrict the reduction within each diffraction-limited focal spot by removing undesired reductions ascribed to the diffusion of cumulative heating, but also enable a finely controllable means of modulating the extent of the reduction for a tunable dispersion by the intensity of the irradiance.

Diffractive photonic applications

As the facile laser reduction method allows exquisite control over both the structures and the compositions of rGO, direct patterning rGO-based photonic devices with tunable physical properties is possible, which is desired for versatile functionalities. With the rapid development of laser-induced reduction of GO, it has motivated broad interests expanding from electronic to optical applications, such as sensors, batteries, photovoltaic devices, and ultrathin polarizers[26,38]. As one crucial branch among these brilliant applications, the diffractive photonic applications of the rGO-based photonic devices are concretely introduced as follows.

Information storage

The need for ever increasing amounts of information storage capacity compels the development of three-dimensional (3D) optical memories based on the localized modulations on physical properties of recording materials such as refractive index and fluorescence[39,40]. The intrinsic fluorescence ranging from the visible to the NIR region makes GO intriguing for applications in 3D

optical data storage. In particular, the deoxygenation by the photoreduction process results in a structural restoration towards graphene and a diminished fluorescence intensity, which therefore provides a stark contrast at the subwavelength scale for recording and retrieving information. A femtosecond-pulsed laser beam with central wavelength around 800 nm was introduced for the nonlinear reduction of fluorescent GO dispersed into a polymer matrix. Figure 4 depicts that photoreduction induced by nonlinear absorption significantly inhibits in the fluorescence intensity from 550 nm to 750 nm of the rGO, as the heterogeneous electronic and atomic structures associated with the oxygen-containing functional groups are gradually removed. Almost completely suppressed fluorescence emission is observed once the laser beam exceeds 8 mW. The spatially confined reduction allows to record multilayer patterns composed of arrays of binary information which can be retrieved back distinctively based on the stark contrast in two-photon fluorescence (Fig. 4a). An equivalent density up to 0.2 Tbits·cm^{-3} has been demonstrated based on the lateral bit size of 1.5 μm and the layer separation of 20 μm[14].

Since the extent of reduction, the atomic structures, the transmission and the extinction coefficients of rGO can be reliably controlled in a reproducible manner by varying pulse energies and exposure times, patterning complex and grayscale photographs is possible. Large scale and high quality GO thin film was prepared through drop-casting onto a LightScribe-enabled DVD disk. By establishing the relationship amongst the decreased transmission in rGO and the laser intensity, different levels of grayscale and black colors can be generated. Employing this facile laser scribing technique, Strong et al. has successfully demonstrated a delicate image of a man's head with circuits, as shown in Fig. 4b[35].

Planar lens

In light of their ultra-compact footprint and high integratability, tremendous research efforts have been devoted to the development of planar lenses, such as plasmonic lenses, superlenses and meta-lenses[41,42]. In this regard, the tunable linear dispersion of patterned rGO realized by direct laser writing techniques could provide a promising platform for light-weight and flexible planar lenses. Zheng et al. demonstrated an ultrathin planar lens patterned in a 200 nm thick GO film, which exhibits far-field 3D subwavelength focusing capability with an efficiency greater than 32% for a broadband ranging from 400 nm to 1500 nm[13]. The exposure of the GO film to the intense femtosecond pulse irradiation leads to a gradual decrease in the film thickness, accompanied by an augment in both refractive index and absorption coefficient.

Figure 5 presents a Fresnel-type planar lens which is composed of several interleaved sub-micrometer concentric rings of GO and rGO. Ideally, the lens design relying on the constructive and destructive interferences within the focal region requires the phase difference between adjacent rGO and GO zones equal to π for a high focusing efficiency. Even though the phase difference is smaller than π, the amplitude modulation resulted from the concomitant augments in extinction coefficients takes the responsibility to intensely enhance the focusing efficiency over a broad bandwidth. Most importantly, the excellent mechanical robustness of GO films maintains the optical performance after bending, making them promising candidates for flexible devices.

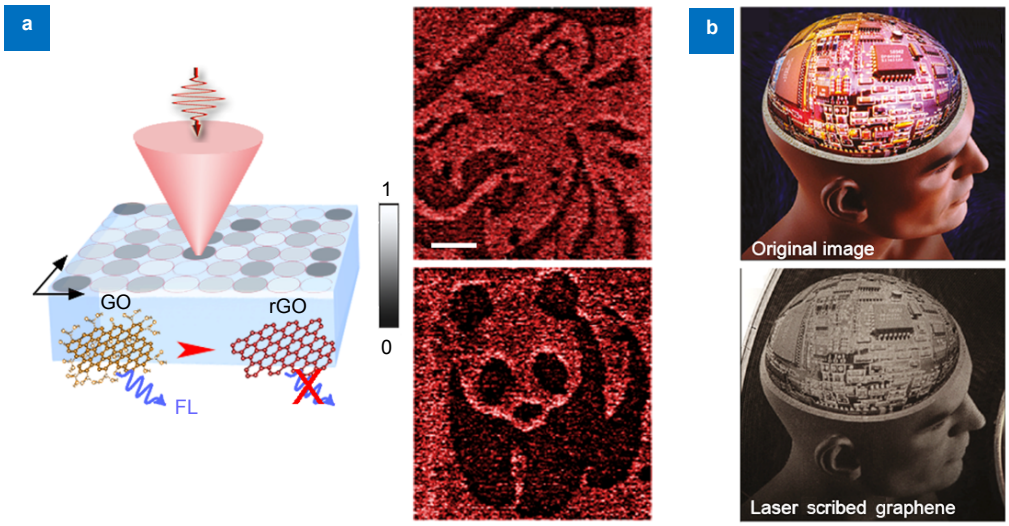

Fig. 4 | (**a**) Retrieved fluorescence image of two patterns recorded through two-photon photoreduction in two layers in GO-polymer sample separated by a spacing of 20 μm. The scale bar is 10 μm. (**b**) A complex grayscale photograph patterned through LightScribe methods. Figure reproduced from: (**a**) ref. [14], Nature Publishing Group; (**b**) ref. [35], American Chemical Society.

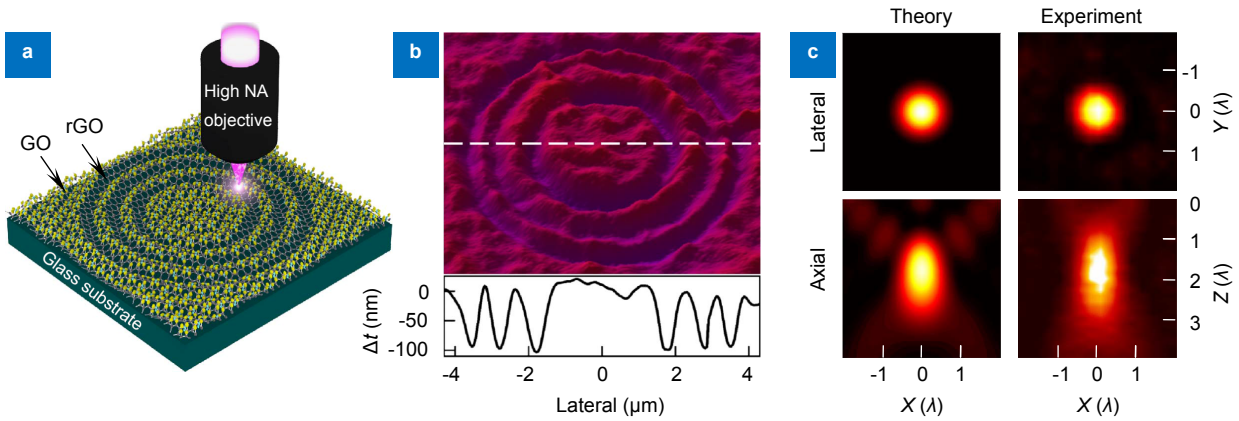

Fig. 5 | (**a**) Schematic illustration of the laser-patterned rGO planar lens. (**b**) Topographic profile of the rGO planar lens prepared by direct laser writing methods. (**c**) Simulated and experimental results of the intensity distributions of the focal field in the lateral and axial directions. Figure reproduced from ref. [13], Springer Nature.

Holographic display

Owing to its capability to mold arbitrary wavefronts with full information including phase and amplitude to reconstruct real 3D images, holographic display has received tremendous research attentions. The continuously tunable phase modulation at the subwavelength scale holds a key to the physical realization of holographic 3D images with high efficiencies and wide angles, which impulses the onrushing development of metasurface holograms based on noble metals[43-45]. The highly spatial confinement and continuously tunable linear dispersion resulted from the controllable reduction by the laser intensities open new avenues for holographic displays based on rGO.

A gigantic refractive index modulation up to 10^{-1} resulted from the intrinsic atomic structure change from GO to rGO has been observed under the irradiance of femtosecond pulses[14,15]. Such a large refractive index increment enables a multilevel phase modulation by exquisitely controlling the irradiance. Computer-generated phase hologram of a planar pattern of a kangaroo is digitalized into arrays of discrete levels according the established relationship of the pulse energies. Then, the phase pattern is recorded by synergistically moving the GO-dispersed sample with respect to the focal spots with variant intensities to produce corresponding phase modulations. The image can be clearly reconstructed with a diffraction efficiency greater than 15% by using a low-power He-Ne laser beam[14].

In addition, the athermal photoreduction by single femtosecond pulses enables a highly spatially confined refractive index change for recorded holograms with a subwavelength scale phase modulation, thus wide viewing angles and full-depth perceptions of the reconstructed image are feasible. A viewing angle up to 52 degrees has been experimentally demonstrated at a pixel size reduced to 0.55 μm, which transcends the current state of the art by liquid-crystal based spatial light modulators by one order of magnitude. The real images of the reconstructed objects, two teapots floating above the rGO hologram, are acquired by the CCD focusing at different depth, as shown in Fig. 6. Remarkably, full color 3D images can be reconstructed based on the appealing feature of the spectrally-insensitive refractive-index modulation of rGO. By utilizing a wavelength-multiplexed phase hologram approach with certain angular offsets at the corresponding wavelengths of 405, 532 and 632 nm, respectively, full-color images can be vividly viewed. Figure 6e depicts the reconstructed image of two balloons composed of primary colors, which are observed vividly from the multiplexed hologram based on rGO[15].

Conclusions and outlook

In this paper, we have reviewed the state-of-the-art developments in laser-reduced GO as well as its applications in photonic devices. By removing the necessity of additional film transfer of prepared rGO to the substrate, the laser reduction method allows in-situ and one-step fabrications of rGO-based devices, which is particularly intriguing. For comparison with other approaches such as chemical or high temperature thermal annealing treatments, the laser reduction method is facile, cost-effective and up-scalable. Even though a rapid development in this field has been achieved, completely restoring the sp2 carbon network and recovering the physical properties of graphene have never been achieved yet by laser reduction methods. This is largely attributed to the structural defects inheriting from the chemically prepared GO, which cannot be cured by laser reduction. Moreover, the complexity and uncertainty of the species and distributions of oxygen-based groups beset the insights and quantified understanding into the structure itself. Nevertheless, the versatile beam parameter control enables to tailor the optoelectronic properties of rGO, such as tunable disper-

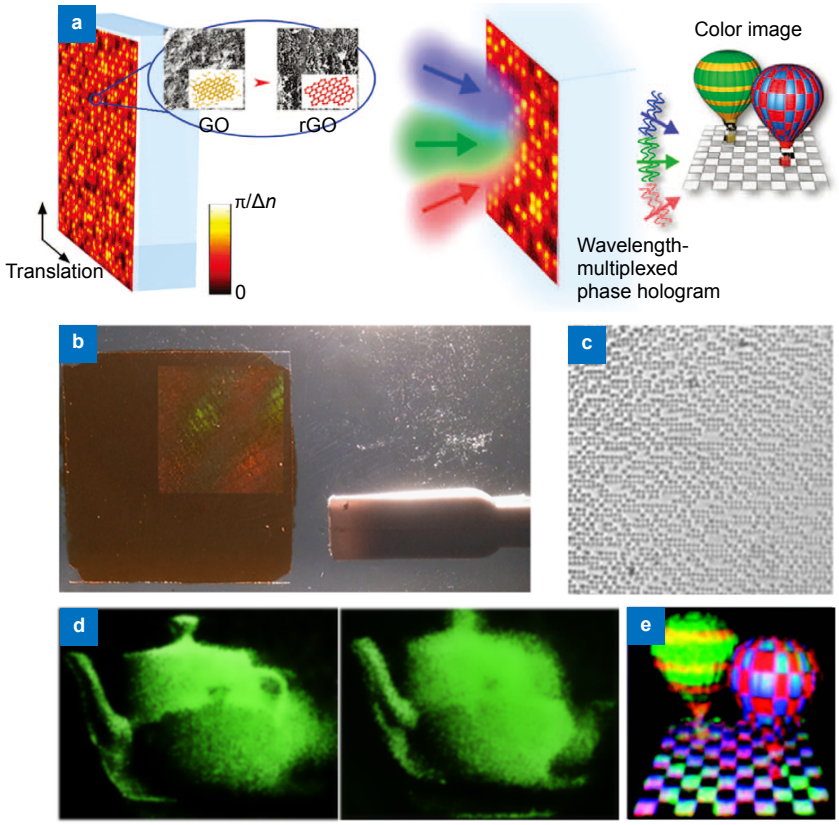

Fig. 6 | (**a**) Schematic illustration of subwavelength scale and continuously tunable phase modulation in rGO holograms for full-color 3D displays achieved by exquisitely controllable photoreduction. (**b**) Photograph of a rGO hologram recorded in a GO-dispersed sample. (**c**) The optical image of the rGO holograms generated by laser reduction. (**d**) CCD-captured images by focusing at different depths of reconstructed 3D objects, two teapots. (**e**) Reconstructed color images of two balloons by rGO-polymer holograms through wavelength multiplexing. Figure reproduced from: (**a**, **b**, **d**, **e**) ref. [15], Springer Nature; (**c**) ref. [14], Nature Publishing Group.

sion and modulated fluorescence, and hence, making it an exceptional integratable platform for the next-generation photonic applications with diverse functionalities[46,47]. Likely, full use of rGO in various scientific and industrial fields with the help of direct laser writing techniques is eminently feasible in the near future.

References

1. Geim A K, Novoselov K S. The rise of graphene. *Nat Mater* **6**, 183–191 (2007).
2. Stankovich S, Dikin D A, Dommett G H B, Kohlhaas K M, Zimney E J *et al*. Graphene-based composite materials. *Nature* **442**, 282–286 (2006).
3. Eda G, Fanchini G, Chhowalla M. Large-area ultrathin films of reduced graphene oxide as a transparent and flexible electronic material. *Nat Nanotechnol* **3**, 270–274 (2008).
4. Zhu Y W, Murali S, Cai W W, Li X S, Suk J W *et al*. Graphene and graphene oxide: synthesis, properties, and applications. *Adv Mater* **22**, 3906–3924 (2010).
5. Eda G, Lin Y Y, Miller S, Chen C W, Su W F *et al*. Transparent and conducting electrodes for organic electronics from reduced graphene oxide. *Appl Phys Lett* **92**, 233305 (2008).
6. Zhang Y L, Guo L, Wei S, He Y Y, Xia H *et al*. Direct imprinting of microcircuits on graphene oxides film by femtosecond laser reduction. *Nano Today* **5**, 15–20 (2010).
7. Li X S, Zhu Y W, Cai W W, Borysiak M, Han B Y *et al*. Transfer of large-area graphene films for high-performance transparent conductive electrodes. *Nano Lett* **9**, 4359–4363 (2009).
8. El-Kady M F, Strong V, Dubin S, Kaner R B. Laser scribing of high-performance and flexible graphene-based electrochemical capacitors. *Science* **335**, 1326–1330 (2012).
9. Gao W, Singh N, Song L, Liu Z, Reddy A L M *et al*. Direct laser writing of micro-supercapacitors on hydrated graphite oxide films. *Nat Nanotechnol* **6**, 496–500 (2011).
10. El-Kady M F, Kaner R B. Scalable fabrication of high-power graphene micro-supercapacitors for flexible and on-chip energy storage. *Nat Commun* **4**, 1475 (2013).
11. Robinson J T, Perkins F K, Snow E S, Wei Z Q, Sheehan P E. Reduced graphene oxide molecular sensors. *Nano Lett* **8**, 3137–3140 (2008).
12. Li W W, Geng X M, Guo Y F, Rong J Z, Gong Y P *et al*. Reduced graphene oxide electrically contacted graphene sensor for highly sensitive nitric oxide detection. *ACS Nano* **5**, 6955–6961 (2011).
13. Zheng X R, Jia B H, Lin H, Qiu L, Li D *et al*. Highly efficient and ultra-broadband graphene oxide ultrathin lenses with three-dimensional subwavelength focusing. *Nat Commun* **6**,

8433 (2015).
14. Li X P, Zhang Q M, Chen X, Gu M. Giant refractive-index modulation by two-photon reduction of fluorescent graphene oxides for multimode optical recording. *Sci Rep* **3**, 2819 (2013).
15. Li X P, Ren H R, Chen X, Liu J, Li Q *et al*. Athermally photoreduced graphene oxides for three-dimensional holographic images. *Nat Commun* **6**, 6984 (2015).
16. Gómez-Navarro C, Meyer J C, Sundaram R S, Chuvilin A, Kurasch S *et al*. Atomic structure of reduced graphene oxide. *Nano Lett* **10**, 1144–1148 (2010).
17. Gao W, Alemany L B, Ci L J, Ajayan P M. New insights into the structure and reduction of graphite oxide. *Nat Chem* **1**, 403–408 (2009).
18. He H Y, Klinowski J, Forster M, Lerf A. A new structural model for graphite oxide. *Chem Phys Lett* **287**, 53–56 (1998).
19. Loh K P, Bao Q L, Eda G, Chhowalla M. Graphene oxide as a chemically tunable platform for optical applications. *Nat Chem* **2**, 1015–1024 (2010).
20. Stankovich S, Dikin D A, Piner R D, Kohlhaas K A, Kleinhammes A *et al*. Synthesis of graphene-based nanosheets via chemical reduction of exfoliated graphite oxide. *Carbon* **45**, 1558–1565 (2007).
21. Dreyer D R, Park S, Bielawski C W, Ruoff R S. The chemistry of graphene oxide. *Chem Soc Rev* **39**, 228–240 (2010).
22. Sun X M, Liu Z, Welsher K, Robinson J T, Goodwin A *et al*. Nano-graphene oxide for cellular imaging and drug delivery. *Nano Res* **1**, 203–212 (2008).
23. Liu Z, Robinson J T, Sun X M, Dai H J. PEGylated nanographene oxide for delivery of water-insoluble cancer drugs. *J Am Chem Soc* **130**, 10876–10877 (2008).
24. Pan D Y, Zhang J C, Li Z, Wu M H. Hydrothermal route for cutting graphene sheets into blue-luminescent graphene quantum dots. *Adv Mater* **22**, 734–738 (2010).
25. Tung V C, Allen M J, Yang Y, Kaner R B. High-throughput solution processing of large-scale graphene. *Nat Nanotechnol* **4**, 25–29 (2009).
26. Zheng X R, Lin H, Yang T S, Jia B H. Laser trimming of graphene oxide for functional photonic applications. *J Phys D Appl Phys* **50**, 074003 (2017).
27. Trusovas R, Račiukaitis G, Niaura G, Barkauskas J, Valušis G *et al*. Recent advances in laser utilization in the chemical modification of graphene oxide and its applications. *Adv Opt Mater* **4**, 37–65 (2016).
28. Robertson J, O'Reilly E P. Electronic and atomic structure of amorphous carbon. *Phys Rev B* **35**, 2946–2957 (1987).
29. Yang D X, Velamakanni A, Bozoklu G, Park S, Stoller M *et al*. Chemical analysis of graphene oxide films after heat and chemical treatments by X-ray photoelectron and Micro-Raman spectroscopy. *Carbon* **47**, 145–152 (2009).
30. Kotov N A, Dékány I, Fendler J H. Ultrathin graphite oxide-polyelectrolyte composites prepared by self-assembly: transition between conductive and non-conductive states. *Adv Mater* **8**, 637–641 (1996).
31. Li X L, Wang H L, Robinson J T, Sanchez H, Diankov G *et al*. Simultaneous nitrogen doping and reduction of graphene oxide. *J Am Chem Soc* **131**, 15939–15944 (2009).
32. Wei Z Q, Wang D B, Kim S, Kim S Y, Hu Y K *et al*. Nanoscale tunable reduction of graphene oxide for graphene electronics. *Science* **328**, 1373–1376 (2010).
33. Zhou Y, Bao Q L, Varghese B, Tang L A L, Tan C K *et al*. Microstructuring of graphene oxide nanosheets using direct laser writing. *Adv Mater* **22**, 67–71 (2010).
34. Zhou Y, Loh K P. Making patterns on graphene. *Adv Mater* **22**, 3615–3620 (2010).
35. Strong V, Dubin S, El-Kady M F, Lech A, Wang Y *et al*. Patterning and electronic tuning of laser scribed graphene for flexible all-carbon devices. *ACS Nano* **6**, 1395–1403 (2012).
36. Trusovas R, Ratautas K, Račiukaitis G, Barkauskas J, Stankevičienė I *et al*. Reduction of graphite oxide to graphene with laser irradiation. *Carbon* **52**, 574–582 (2013).
37. Smirnov V A, Arbuzov A A, Shul'ga Y M, Baskakov S A, Martynenko V M *et al*. Photoreduction of graphite oxide. *High Energy Chem* **45**, 57–61 (2011).
38. Zhang Y L, Guo L, Xia H, Chen Q D, Feng J *et al*. Photoreduction of graphene oxides: methods, properties, and applications. *Adv Opt Mater* **2**, 10 (2014).
39. Li X P, Lan T H, Tien C H, Gu M. Three-dimensional orientation-unlimited polarization encryption by a single optically configured vectorial beam. *Nat Commun* **3**, 998 (2012).
40. Li X P, Cao Y Y, Gu M. Superresolution-focal-volume induced 3.0 Tbytes/disk capacity by focusing a radially polarized beam. *Opt Lett* **36**, 2510–2512 (2011).
41. Kawata S, Inouye Y, Verma P. Plasmonics for near-field nano-imaging and superlensing. *Nat Photonics* **3**, 388–394 (2009).
42. Khorasaninejad M, Chen W T, Devlin R C, Oh J, Zhu A Y *et al*. Metalenses at visible wavelengths: diffraction-limited focusing and subwavelength resolution imaging. *Science* **352**, 1190–1194 (2016).
43. Zheng G X, Mühlenbernd H, Kenney M, Li G X, Zentgraf T *et al*. Metasurface holograms reaching 80% efficiency. *Nat Nanotechnol* **10**, 308–312 (2015).
44. Huang L Q, Chen X Z, Mühlenbernd H, Zhang H, Chen S M *et al*. Three-dimensional optical holography using a plasmonic metasurface. *Nat Commun* **4**, 2808 (2013).
45. Li X, Chen L W, Li Y, Zhang X H, Pu M B *et al*. Multicolor 3D meta-holography by broadband plasmonic modulation. *Sci Adv* **2**, e1601102 (2016).
46. Ren H R, Li X P, Zhang Q M, Gu M. On-chip noninterference angular momentum multiplexing of broadband light. *Science* **352**, 805 (2016).
47. Li X P, Liu J, Cao L C, Wang Y T, Jin G F *et al*. Light-control-light nanoplasmonic modulator for 3D micro-optical beam shaping. *Adv Opt Mater* **4**, 70–75 (2016).

Acknowledgements

The authors thank National Natural Science Foundation of China (61522504, 61420106014, 61432007, 11604123) and Guangdong Provincial Innovation and Entrepreneurship Project (2016ZT06D081) for funding supports. M Gu acknowledges the supports from the Australian Research Council (ARC) through the Discovery Project (DP140100849) and Laureate Fellowship Scheme (FL100100099).

Competing interests

The authors declare no competing financial interests.